July 30, 2004

Application of the Carr–Purcell Meiboom–Gill Pulse Sequence for the Acquisition of Solid-State NMR Spectra of Spin-1/2 Nuclei

Ivan Hung, *University of Windsor*
Aaron J. Rossini, *University of Windsor*
Robert W. Schurko, *University of Windsor*

Application of the Carr−Purcell Meiboom−Gill Pulse Sequence for the Acquisition of Solid-State NMR Spectra of Spin-$^1/_2$ Nuclei

Ivan Hung, Aaron J. Rossini, and Robert W. Schurko*

Department of Chemistry and Biochemistry, University of Windsor, 401 Sunset Avenue, Windsor, Ontario, Canada N9B 3P4

Received: February 9, 2004; In Final Form: June 1, 2004

The quadrupolar Carr−Purcell Meiboom−Gill (QCPMG) pulse sequence has received much attention in the recent literature for use in the rapid acquisition of solid-state NMR spectra of half-integer quadrupolar nuclei. Herein we investigate the application of the CPMG pulse sequence to enhance the signal-to-noise ratio in the static NMR spectra of spin-$^1/_2$ nuclei. CPMG is coupled with techniques such as cross-polarization (CP) and two-pulse phase-modulated (TPPM) proton decoupling. The CPMG and CP/CPMG pulse sequences are applied to a series of different NMR nuclides, including ^{113}Cd, ^{199}Hg, ^{207}Pb, ^{15}N and ^{109}Ag. Standard ^{113}Cd CP/MAS, MAS and static NMR spectra of $Cd(NO_3)_2{\cdot}4H_2O$ are compared with corresponding ^{113}Cd CPMG and CP/CPMG NMR spectra. Piecewise-acquired wide-line CPMG ^{199}Hg and ^{207}Pb NMR spectra of $(CH_3COO)_2Hg$ and $(CH_3COO)_2Pb{\cdot}3H_2O$, which are so broad that they cannot be uniformly excited by a single short pulse, reveal that chemical shielding tensor parameters can be determined from these rapidly acquired spectra more accurately than with corresponding CP/MAS spectra. CP/CPMG NMR is also applied to acquire NMR spectra of low-γ nuclei such as ^{15}N in $^{15}NH_4{}^{15}NO_3$ (98%-enriched) and ^{109}Ag in $AgSO_3CH_3$. The signal obtained from CPMG NMR experiments on stationary samples is comparable to corresponding MAS spectra and much higher than for conventional static NMR spectra, providing an interesting alternative for investigating spin-$^1/_2$ nuclei with broad powder patterns.

Introduction

A large number of solid-state NMR studies on materials containing unreceptive nuclei have recently been published due to the increasing availability of high magnetic fields, sophisticated NMR hardware, and the development of new pulse sequences and methodologies for acquiring NMR spectra of low-γ nuclei.[1,2] Unreceptive nuclei are nuclei that are not amenable to standard NMR experiments owing to (i) low magnetogyric ratios (γ), (ii) low natural abundances, (iii) large nuclear quadrupole moments (in the case of quadrupolar nuclei), (iv) dilution of the nuclide of interest, (v) lengthy longitudinal relaxation times, (vi) exceedingly broad powder patterns, or (vii) any combination of the above properties. Common means of circumventing such difficulties include running NMR experiments at ultrahigh magnetic field strengths, at very low temperatures (e.g., below 50 K) and/or employing isotopic labeling. However, many of these measures are costly to the point of being prohibitive for many scientists interested in routinely conducting solid-state NMR experiments on unreceptive nuclei.

Recently, the quadrupolar Carr−Purcell Meiboom−Gill (QCPMG) sequence was introduced as a means of enhancing signal intensity in the NMR spectra of half-integer quadrupolar nuclei (i.e., nuclear spins of $^3/_2$, $^5/_2$, $^7/_2$ and $^9/_2$).[3] The QCPMG sequence is very similar to the traditional CPMG sequence utilized for measuring transverse relaxation time constants.[4] The QCPMG sequence (Figure 1a) consists of a single $\pi/2$ pulse followed by a train of alternating π pulses (which produce spin−echoes) and detection periods (in which the echo FIDs are acquired and stored). By acquisition of the spin−echoes multiple times within a single scan, large signal enhancements can be obtained over the course of an experiment, making this technique advantageous for all types of unreceptive nuclei. The QCPMG FID consists of a series of echoes in the time domain which may be Fourier transformed to produce a manifold of "spikelets" in the frequency domain. For most half-integer quadrupolar nuclei, the shape of this manifold corresponds to the shape of the central-transition powder pattern. The timing of the pulse sequence can be adjusted to produce a train of echoes with variable spacing in the time domain, such that close spacing in the time domain leads to a spectrum of high signal intensity

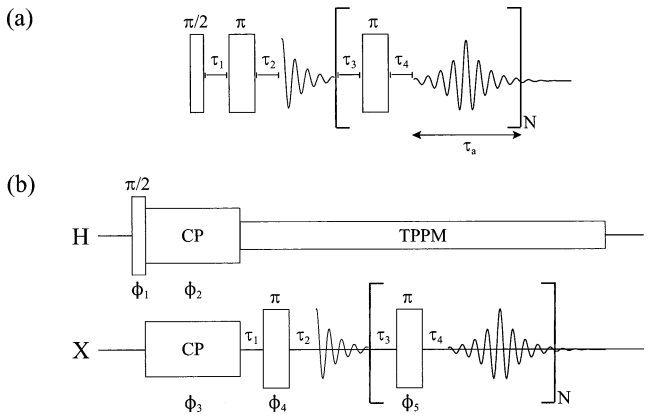

Figure 1. Schematics of the (a) (Q)CPMG and (b) CP/CPMG with TPPM decoupling pulse sequences. The phases for each of the pulses in the CP/CPMG sequence are: $\phi_1 = 2, 0, 0, 2$; $\phi_2 = 1$; $\phi_3 = 3, 2$; $\phi_4 = 1, 0, 1, 0, 3, 2, 3, 2$; $\phi_5 = 1, 0, 1, 0, 3, 2, 3, 2, 3, 2, 3, 2, 1, 0, 1, 0$; with receiver phase list $\phi_r = (2, 3, 0, 1) \times 4$, where $\{n\pi/2 | n = 0, 1, 2, 3\}$.

* To whom correspondence may be addressed. Email: rschurko@uwindsor.ca. Web: http://www.uwindsor.ca/schurko.

10.1021/jp0401123 CCC: $27.50
Published on Web 07/30/2004

TABLE 1: Nuclear Properties of Studied Nuclei

nucleus	natural abundance (%)	γ (10^7 rad s^{-1} T^{-1})	ν_0 (MHz) at $B_0 = 9.4$ T	T_1 (s)[a]	^{1}H T_1 (s)[b]
^{15}N	0.37	−2.7126	40.52		
^{109}Ag	48.18	−1.2519	18.60		<5[c]
^{113}Cd	12.26	−5.9609	88.65	>300[d]	<0.5[d]
^{199}Hg	16.84	4.8458	71.42	290[e]	25[e]
^{207}Pb	22.60	5.6264	83.47		0.56[f]

[a] Spin−lattice relaxation time of relevant nuclei in compounds studied. [b] Hydrogen spin−lattice relaxation times in studied compounds. [c] Reference 29. [d] Reference 34. [e] Reference 40. [f] Reference 49.

but low resolution and far spacing leads to the opposite situation. The echoes from a CPMG train may be co-added to produce a central transition pattern of increased intensity compared to the standard Hahn-echo pattern or processed with sawtooth apodization functions.[5]

The QCPMG sequence has been applied to quadrupolar nuclei in stationary samples and under conditions of magic-angle spinning (MAS) in a number of standard samples[3] and interesting biological,[6,7] organic,[8] organometallic[9] and inorganic materials.[10] QCPMG has also been utilized as a means of detecting the direct dimension in the MQMAS experiment (which is used for obtaining high-resolution NMR spectra of half-integer quadrupolar nuclei)[11] and has been implemented in wide-line piecewise acquisitions of spectra of quadrupolar nuclei with powder patterns exceeding standard excitation bandwidth.[7] Cross-polarization (CP) QCPMG sequences have been used to acquire spectra of half-integer nuclei in proton-containing systems,[2] and amplitude-modulated double-frequency sweep (DFS) and rotor assisted population transfer (RAPT) pulse sequences have been coupled with the QCPMG sequence as preparatory sequences for further signal enhancements.[12]

An interesting application of the QCPMG sequence for signal enhancement was reported by Farnan and co-workers in an ^{17}O and ^{29}Si NMR study of α-cristobalite.[13] The QCPMG sequence was applied to obtain high quality ^{17}O (spin = $^5/_2$) MAS NMR spectra, but also of interest was the application of the pulse sequence to acquire the ^{29}Si (spin = $^1/_2$) NMR spectra. The ^{29}Si NMR resonances in question are quite broad due to chemical shift distributions which result from the amorphous nature of the materials under examination. The implications of these experiments are significant, since there are many spin-$^1/_2$ nuclei that have broad powder patterns resulting from large chemical shift anisotropy, chemical shift distributions, or other line-broadening mechanisms.[14,15] Many of these spin-$^1/_2$ nuclei also have low natural abundances, low magnetogyric ratios, and/or long spin−lattice relaxation times (T_1). The work of Farnan et al. is not the only application of CPMG-type sequences to spin-$^1/_2$ nuclei but rather one that closely resembles the recent QCPMG work in the literature. Aside from the typical use of the CPMG-type sequences to measure spin−spin relaxation time constants, they have also been used to enhance the ^{89}Y NMR signal of $YBa_2Cu_3O_{7-\delta}$,[16] study dipolar-induced spin−lattice relaxation,[17] enhance signal within the magic-angle hopping experiment,[18] double-quantum NMR experiments,[19] and the MEPHORMAT sequence,[20] as well as for resolving dipolar splittings between nuclei such as ^{1}H and ^{19}F.[21]

In this paper, we present examples of the CPMG pulse sequence applied to the study of five different nuclei: ^{113}Cd, ^{199}Hg, ^{207}Pb, ^{15}N and ^{109}Ag (Table 1). The CPMG NMR spectra of stationary samples of $Cd(NO_3)_2{\cdot}4H_2O$, $(CH_3COO)_2Hg$, $(CH_3COO)_2Pb{\cdot}3H_2O$, doubly labeled $^{15}NH_4{}^{15}NO_3$ and $AgSO_3CH_3$ are presented. CP/CPMG NMR spectra are acquired with high-power two-pulse phase modulated (TPPM) proton-decoupling[22] throughout the train of π pulses and acquisition periods. Comparison of the CPMG and CP/CPMG spectra with conventional MAS and CP/MAS NMR spectra are presented. Full details of experimental parameters used in each experiment are also provided. The aim of this work is to demonstrate that the CPMG sequence can be used to acquire high-quality static spectra of spin-$^1/_2$ nuclei with broad powder patterns arising from chemical shielding anisotropy (CSA) or other sources of line-broadening efficiently. Notably, this sequence is useful for samples with long spin−lattice relaxation times, unusual spinning speed-dependent CP behavior, low NMR frequencies, low natural abundances, or a combination of these factors.

Experimental Section

Samples of ammonium nitrate ($^{15}NH_4{}^{15}NO_3$, 98% ^{15}N), silver methanesulfonate ($AgSO_3CH_3$), cadmium nitrate tetrahydrate ($Cd(NO_3)_2{\cdot}4H_2O$), and mercury(II) acetate ($(CH_3COO)_2Hg$) were purchased from Sigma-Aldrich Canada, Ltd., and used without further purification. Lead(II) acetate trihydrate ($(CH_3COO)_2Pb{\cdot}3H_2O$) was obtained from the same company and recrystallized from aqueous solution, since it has been shown by ^{13}C CP/MAS NMR that $(CH_3COO)_2Pb{\cdot}3H_2O$ undergoes dehydration and phase transformation over time at room temperature.[23] ^{207}Pb NMR spectra of a mixture of pure lead acetate trihydrate and the partially or completely dehydrated lead acetate are shown in the Supporting Information (Figure 1S). Samples were finely powdered and packed into 4 mm outer diameter zirconia rotors for ^{15}N and ^{109}Ag experiments and 5 mm outer diameter rotors for ^{113}Cd, ^{199}Hg and ^{207}Pb experiments.

Solid-state NMR spectra were acquired on a Varian Infinity Plus NMR Spectrometer with an Oxford 9.4 T ($\nu_0(^1H) = 400$ MHz) wide-bore magnet operating at $\nu_0(^{15}N) = 40.52$ MHz, $\nu_0(^{109}Ag) = 18.60$ MHz, $\nu_0(^{113}Cd) = 88.65$ MHz, $\nu_0(^{199}Hg) = 71.42$ MHz and $\nu_0(^{207}Pb) = 83.47$ MHz. When working at the low ^{109}Ag Larmor frequency, high forward-to-reflected power was achieved by employing a Varian/Chemagnetics Low Gamma Tuning Box.

^{113}Cd chemical shifts are reported with respect to an external saturated solution of $Cd(NO_3)_2{\cdot}4H_2O$ with its isotropic shift (δ_{iso}) set to 0.0 ppm, though an alternative referencing system features setting $\delta_{iso} = -102.2$ ppm for solid $Cd(NO_3)_2{\cdot}4H_2O$ with respect to solid $Cd(ClO_4)_2$.[24] ^{199}Hg chemical shifts were referenced to $Hg(CH_3)_2$ ($\delta_{iso} = 0.0$ ppm) by setting the chemical shift of a concentrated $Hg(ClO_4)_2$ aqueous solution to −2253 ppm.[25] ^{207}Pb NMR spectra were referenced to $Pb(CH_3)_2$ by setting an external 0.5 M aqueous solution of $Pb(NO_3)_2$ to $\delta_{iso} = -2941$ ppm.[26] Nitrogen chemical shifts were referenced to liquid ammonia at 20 °C by setting the isotropic shift of the ammonium resonance in $^{15}NH_4{}^{15}NO_3$ to 23.8 ppm.[27,28] The ^{109}Ag shift of $AgSO_3CH_3$(s) was set to $\delta_{iso} = 87.2$ ppm, such that it is referenced to 9 M $AgNO_3$(aq) at $\delta_{iso} = 0.0$ ppm.[29]

Spectral widths of 40, 50, 80, 400 and 400 kHz were employed for ^{15}N, ^{109}Ag, ^{113}Cd, ^{199}Hg and ^{207}Pb experiments, respectively. Intervals of 12, 5, 30, 90 and 4 s were used between acquisitions for all ^{15}N, ^{109}Ag, ^{113}Cd, ^{199}Hg and ^{207}Pb CP

experiments, while for ^{113}Cd, ^{199}Hg and ^{207}Pb non-CP experiments, intervals of 60, 1450 and 20 s were employed. For ^{113}Cd, ^{199}Hg and ^{207}Pb non-CP NMR spectra, $\pi/2$ pulses of 4.4, 3.1 and 3.0 μs with radio frequency (rf) fields of $\nu_1 = 56.8$, 80.6 and 83.3 kHz were utilized, respectively, along with corresponding π pulses (where applicable). The TPPM heteronuclear decoupling scheme[22] was employed in all cases with typical ^{1}H decoupling field strengths of 13−29 kHz.

^{15}N CP NMR spectra were acquired with a 35 ms contact time (ct), a proton $\pi/2$ pulse ($\tau^{H}_{\pi/2}$) of 2.87 μs, a rf field of $\nu_{1H} = 87.1$ kHz, and matched radio frequency fields (ν_{CP}) of 58.4 kHz for CP. ^{15}N CP/Hahn-echo and CP/CPMG experiments employed a π pulse of 6.6 μs and a rf field of 75.8 kHz. Furthermore, interpulse (τ_1, τ_3) and preacquisition (τ_2, τ_4) periods of 60 μs, 408 Meiboom−Gill (MG) loops and an acquisition time per echo (τ_a) of 2.0 ms were employed for the CP/CPMG experiment, while $\tau_1 = 75$ μs and $\tau_2 = 25$ μs were used for the CP/Hahn-echo spectrum. In particular, $1/\tau_a$ represents the interspikelet separation in the frequency domain of CPMG type spectra. The CP/CPMG sequence is shown in Figure 1b with phase cycling details given in the figure caption.

^{109}Ag CP experiments employed $\tau^{H}_{\pi/2} = 2.8$ μs, $\nu_{1H} = 89.3$ kHz, ct = 40 ms and $\nu_{CP} = 31.6$ kHz. The ^{109}Ag CP/Hahn-echo spectrum was acquired with a 13.5 μs π pulse, rf field of 37.0 kHz, $\tau_1 = 300$ μs and $\tau_2 = 160$ μs, while the CP/CPMG experiment employed MG = 162, $\tau_1 = \tau_2 = 300$ μs, $\tau_3 = \tau_4 = 250$ μs, $\tau_a = 2.0$ ms and the same π pulse.

For ^{113}Cd CP spectra, $\tau^{H}_{\pi/2} = 5.7$ μs, $\nu_{1H} = 43.9$ kHz, ct = 6 ms and $\nu_{CP} = 63.6$ kHz. For both CP and non-CP ^{113}Cd Hahn-echo and CPMG experiments, a π pulse of 8.8 μs and rf field of 56.8 kHz were employed. Further, $\tau_1 = 77.5$ μs and $\tau_2 = 40.0$ μs for the Hahn-echo spectra, and MG = 101, $\tau_a = 0.5$ ms and $\tau_1 = \tau_2 = \tau_3 = \tau_4 = 70$ μs for the CPMG experiments.

The ^{199}Hg CP/MAS spectrum at 3 kHz spinning frequency (ν_{rot}) was acquired with $\tau^{H}_{\pi/2} = 6.5$ μs, $\nu_{1H} = 38.5$ kHz, ct = 32 ms and $\nu_{CP} = 42.9$ kHz, while the CP/Hahn-echo and CP/CPMG were recorded with $\tau^{H}_{\pi/2} = 2.5$ μs, $\nu_{1H} = 100$ kHz, ct = 32 ms and $\nu_{CP} = 48.6$ kHz. For both the ^{199}Hg CPMG and CP/Hahn-echo experiments, a 6.2 μs π pulse and 80.6 kHz rf field were employed, while for the CP/CPMG spectrum, a π pulse of 11.5 μs and rf field of 43.5 kHz were used. The CPMG experiments were recorded with MG = 247, $\tau_1 = \tau_2 = \tau_3 = \tau_4 = 20$ μs and $\tau_a = 330$ μs, the Hahn-echo spectrum with $\tau_1 = 60$ μs and $\tau_2 = 20$ μs, and each piece of the wide-line CP/CPMG spectrum with MG = 81, $\tau_1 = \tau_2 = \tau_3 = \tau_4 = 20$ μs, and $\tau_a = 250$ μs. The transmitter frequency was varied and retuned through the 71.471−71.331 MHz and 71.440−71.343 MHz frequency ranges in 28 and 48.5 kHz steps for acquisition of the ^{199}Hg wide-line CP/CPMG and CPMG spectra, respectively.

For ^{207}Pb CP/CPMG spectra, $\tau^{H}_{\pi/2} = 3.5$ μs, $\nu_{1H} = 71.4$ kHz, ct = 2 ms and $\nu_{CP} = 35$ kHz were employed along with MG = 326, $\tau_1 = \tau_2 = \tau_3 = \tau_4 = 40$ μs and $\tau_a = 250$ μs. Similar parameters were employed for the CPMG experiment except for pulses and the rf field, which were already mentioned earlier in the Experimental Section. Similar to the ^{199}Hg wide-line CP/CPMG spectrum, the ^{207}Pb wide-line CPMG and CP/CPMG spectra were acquired in 40 kHz steps within the 83.387−83.547 MHz transmitter frequency range.

Simulations of static NMR spectra were accomplished with the WSOLIDS software package, which was written and developed by K. Eichele in R. E. Wasylishen's laboratory at Dalhousie University. Manifolds of spinning sidebands were analyzed using the method of Herzfeld and Berger,[30] which is incorporated into the aforementioned software. Spectra obtained from co-addition of the time-domain spin−echoes and subsequent Fourier transformation generally resemble the envelope of CPMG echo spikelet spectra, which in turn resemble conventional Hahn echo spectra (Supporting Information, Figure 2S). Consequently, extraction of CSA parameters from CPMG spectra was simply accomplished by analytical simulation of their envelopes.

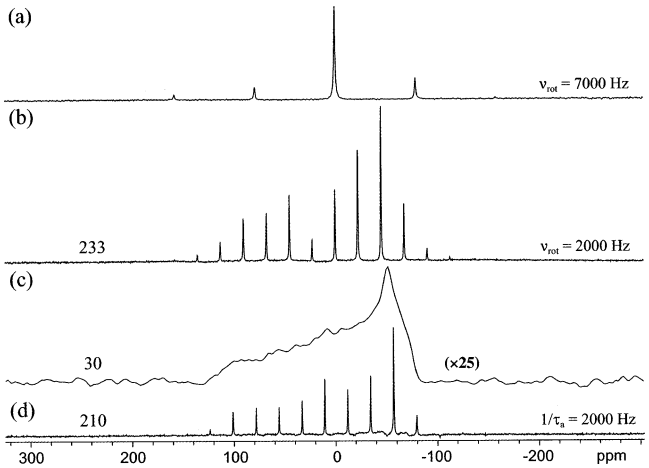

Figure 2. ^{113}Cd CP/MAS at (a) $\nu_{rot} = 7000$ Hz and (b) $\nu_{rot} = 2000$ Hz, (c) static CP/Hahn-echo and (d) static CP/CPMG ($1/\tau_a = 2000$ Hz) NMR spectra of $Cd(NO_3)_2 \cdot 4H_2O$; all recorded with a total of 16 transients. Scaling factors used in modifying the vertical scale of spectra are shown in parentheses; otherwise, all spectra are shown on the same scale. The relevant S/N ratios are shown at the left of each spectrum.

Results and Discussion

The results and discussion are presented in five different subsections divided by nuclei. The ^{113}Cd NMR spectra of $Cd(NO_3)_2 \cdot 4H_2O$ are examined first owing to the high receptivity of ^{113}Cd, the relatively narrow pattern and good CP efficiency. Then, the performance of the CP/CPMG pulse sequence is described for the ^{199}Hg NMR of $(CH_3COO)_2Hg$ and ^{207}Pb NMR of $(CH_3COO)_2Pb \cdot 3H_2O$. Spectra of these nuclei typically have very broad powder patterns influenced by large CSA, and are often very difficult to acquire due to very long spin−lattice relaxation times. Application of the CP/CPMG pulse sequence to unreceptive nuclei with low Larmor frequencies and/or low natural abundances (^{15}N and ^{109}Ag) is then discussed.

^{113}Cd NMR. ^{113}Cd NMR is quite common for the study of Cd coordination compounds as well as the investigation of model biological systems;[31] the latter is notably important due to the use of the receptive ^{113}Cd nucleus as a surrogate for the unreceptive ^{67}Zn nucleus.[32] Solid-state ^{113}Cd NMR studies are often aimed at characterizing cadmium chemical-shielding tensors,[33] which lend insight into the relationship between cadmium coordination environments and experimental cadmium chemical shifts. Initial ^{113}Cd solid-state NMR experiments on $Cd(NO_3)_2 \cdot 4H_2O$ were reported by Gerstein and co-workers in 1980,[34] and later studies were reported by two other groups.[24,35] ^{113}Cd{^{1}H} CP/MAS NMR experiments are preferable to MAS NMR experiments due to long ^{113}Cd spin−lattice relaxation times of close to 300 s, as well as the potential sensitivity enhancement afforded by ^{1}H−^{113}Cd cross polarization.

In parts a and b of Figure 2, ^{113}Cd CP/MAS NMR spectra of $Cd(NO_3)_2 \cdot 4H_2O$ are shown at spinning speeds of 7 and 2 kHz, respectively. Acquisitions of spectra at two spinning speeds are used to identify the isotropic chemical shift and to obtain anisotropic chemical shielding parameters by Herzfeld-Berger

TABLE 2: Anisotropic Chemical Shielding Parameters of Compounds Investigated

compound	experiment	δ_{iso} (ppm)[a]	Ω (ppm)[b]	κ[c]	δ_{11} (ppm)[d]	δ_{22} (ppm)	δ_{33} (ppm)
$Cd(NO_3)_2{\cdot}4H_2O$	CP/MAS (ν_{rot} = 7000 Hz)	0	159	−1.00	106(3)	−53(3)	−53(3)
	CP/MAS (ν_{rot} = 2000 Hz)	0	175	−0.84	112(2)	−49(2)	−63(2)
	CP/Hahn-echo	0	205	−0.75	128(2)	−51(2)	−77(2)
	CP/CPMG	−4	205	−0.78	125(5)	−57(5)	−83(5)
	MAS (ν_{rot} = 2000 Hz)	0	209	−0.73	130(3)	−51(3)	−79(3)
	Hahn-echo	0	200	−0.80	127(4)	−53(4)	−73(4)
	CPMG	−4	205	−0.78	125(5)	−57(5)	−83(5)
	single-crystal[e]	0	196.6	−0.80	124.4	−52.1	−72.2
$(CH_3COO)_2Hg$	CP/MAS (ν_{rot} = 3000 Hz)	−2488	1770	0.87	−1860(40)	−1975(40)	−3630(40)
	wide-line CP/CPMG	−2496	1850	0.87	−1840(30)	−1957(30)	−3690(30)
	MAS (ν_{rot} = 3000 Hz)	−2495	1810	0.86	−1850(30)	−1975(30)	−3660(30)
	CPMG	−2508	1810	0.88	−1870(30)	−1975(30)	−3680(30)
	CP/MAS (ν_{rot} = 3100 Hz)[f]	−2497	1826	0.90	−1859	−1947	−3685
$(CH_3COO)_2Pb{\cdot}3H_2O$	wide-line CP/CPMG	−1881	1690	0.65	−1220(10)	−1513(10)	−2910(10)
	wide-line CPMG	−1898	1693	0.60	−1220(10)	−1561(10)	−2913(10)
	MAS (ν_{rot} = 7000 Hz)	−1868	1590	0.63	−1241(5)	−1532(5)	−2832(5)
	Hahn-echo[g]	−1904	1728	0.62	−1217	−1549	−2945
NH_4NO_3	CP/MAS (ν_{rot} = 5300 Hz)	377	220	0.96	452(3)	447(3)	232(3)
	CP/MAS (ν_{rot} = 500 Hz)	377	216	0.58	464(2)	419(2)	248(2)
	CP/Hahn-echo	377	232	0.72	465(1)	433(1)	233(1)
	CP/CPMG	377	235	0.68	468(2)	430(2)	233(2)
	CP[h]	363	222	0.77	446	420	224
$AgSO_3CH_3$	CP/MAS (ν_{rot} = 500 Hz)	87	197	−0.50	202(5)	54(5)	5(5)
	CP/Hahn-echo	82	192	−0.30	187(3)	63(3)	−5(3)
	CP/CPMG ($1/\tau_a$ = 500 Hz)	80	218	−0.49	207(4)	45(4)	−11(4)
	CP/CPMG ($1/\tau_a$ = 200 Hz)	80	219	−0.45	206(4)	47(4)	−13(4)
	CP[i]	87.2	183	−0.39	191	63	8

[a] Isotropic shift, $\delta_{iso} = (\delta_{11} + \delta_{22} + \delta_{33})/3$. [b] Span of the CS tensor, $\Omega = \delta_{11} - \delta_{33}$. [c] CS tensor skew, $\kappa = 3(\delta_{22} - \delta_{iso})/\Omega$. [d] CS tensor principal components where $\delta_{11} \geq \delta_{22} \geq \delta_{33}$. [e] Reference 24. [f] Reference 40. [g] Reference 48. [h] Reference 61. [i] Reference 29.

analysis. Cadmium CS tensors obtained from analysis of the various types of NMR spectra are shown in Table 2. A ^{113}Cd CP/Hahn-echo NMR spectrum (Figure 2c) is required to obtain an accurate CS pattern for the stationary sample, since standard static CP experiments result in missing points at the beginning of the FID, which lead to baseline distortions in the experimental powder patterns. Cadmium CS parameters obtained from experiments on stationary samples (e.g., $\delta_{iso} = -4$ ppm, $\Omega =$ 205 ppm, $\kappa = -0.78$, see Table 2 for definition of CS parameters) are in good agreement with parameters obtained from single-crystal ^{113}Cd NMR,[24] while the values obtained from Herzfeld−Berger analysis of ^{113}Cd CP/MAS or MAS spectra are also comparable. Increasingly accurate CS tensor parameters can indeed be deduced from simulations of static NMR spectra; however, acquisition of high signal-to-noise (S/N) static spectra often requires long experimental times. Although the static ^{113}Cd CP/CPMG (Figure 2d) and CP/Hahn-echo spectra have been acquired over the same amount of time, the S/N in the former (210) is comparable to the CP/MAS (233) spectrum pictured in Figure 2b, while the latter (30) is much less intense (the S/N ratio for the most intense peak or discontinuity is shown to the left of each spectrum). The gain in S/N comes at the cost of resolution; however, the manifold of "echo-spikelets" in the CP/CPMG spectrum still closely resemble the static ^{113}Cd NMR pattern. We note that it is quite difficult to make precise quantitative comparisons of signal enhancement between static, CP/MAS and CPMG spectra, owing to changes in CP conditions and variation in spectral parameters such as dwell times, acquisition times, total number of points, etc.

Suitable conditions for cross polarization are often not available for many samples. Unfortunately, the long spin−lattice relaxation times encountered for many nuclei in systems of this sort result in very long overall experimental times and poor S/N. For example, the ^{113}Cd CP NMR spectra shown in Figure 2 were acquired in 8 min, whereas the corresponding NMR spectra obtained without CP (Figure 3) required 164 min to obtain

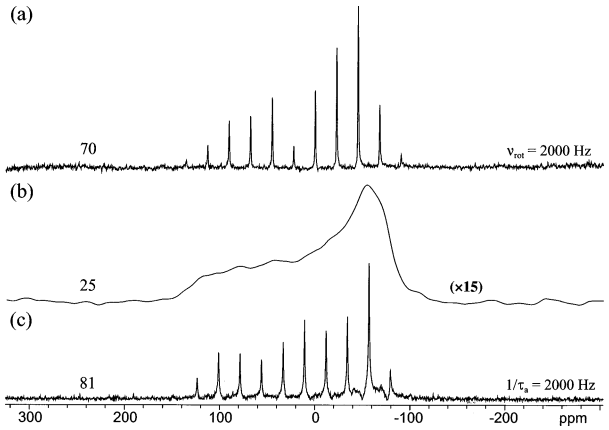

Figure 3. ^{113}Cd (a) MAS at ν_{rot} = 2000 Hz, (b) Hahn-echo and (c) CPMG ($1/\tau_a$ = 2000 Hz) NMR spectra of $Cd(NO_3)_2{\cdot}4H_2O$; 164 transients were averaged for all three spectra.

comparable S/N ratios. In parts a and b of Figure 3, standard ^{113}Cd MAS and static NMR spectra are shown. The corresponding CPMG spectrum (Figure 3c) was acquired under nonspinning conditions, but has slightly superior S/N compared to the MAS NMR spectrum (81 and 70, respectively). The CPMG experiment is potentially very useful for obtaining high S/N spectra of stationary samples; however, it has the disadvantage that isotropic shifts for samples with multiple Cd sites cannot be differentiated (in contrast to MAS NMR experiments). It is possible that the combination of MAS and stationary CPMG experiments may be useful in acquiring isotropic chemical shifts and accurate CS tensor parameters for samples with multiple sites.

^{199}Hg NMR. Solid-state ^{199}Hg NMR studies used to be uncommon owing to the large CSA associated with linear mercury(II) compounds and long spin−lattice relaxation time constants.[36,37] Harris and Sebald first suggested $(CH_3COO)_2Hg$ as a standard setup sample for optimizing ^{199}Hg CP/MAS NMR

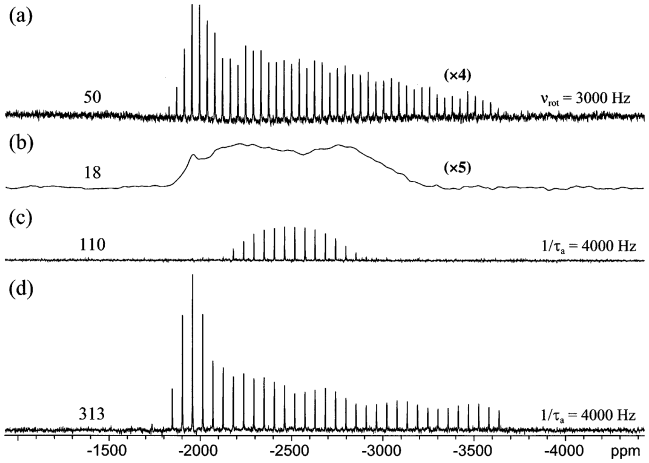

Figure 4. ^{199}Hg (a) CP/MAS at $\nu_{rot} = 3000$ Hz, (b) CP/Hahn-echo, (c) CP/CPMG ($1/\tau_a = 4000$ Hz) and (d) piecewise wide-line CP/CPMG ($1/\tau_a = 4000$ Hz) NMR spectra of $(CH_3COO)_2Hg$. Sixteen transients were recorded for the CP/MAS spectrum and CP/CPMG sub-spectra, while 160 transients were acquired for the CP/Hahn-echo spectrum.

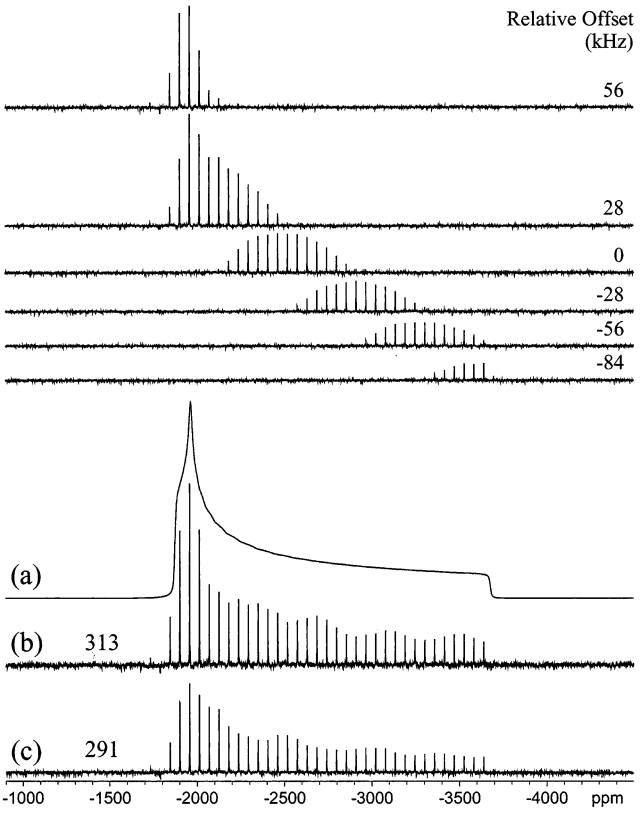

Figure 5. ^{199}Hg wide-line CP/CPMG ($1/\tau_a = 4000$ Hz) spectra of $(CH_3COO)_2Hg$ along with (a) analytical simulation of the spectral envelope. Sub-spectra (top of figure) were acquired by varying the transmitter frequency in 28 kHz steps, where 16 transients were acquired for each sub-spectrum. The ^{199}Hg wide-line CP/CPMG spectra were obtained by (b) addition and (c) taking the skyline projection of the individual segments in the frequency domain.

experiments;[14] they reported two closely spaced isotropic ^{199}Hg resonances for this sample. Santos et al. used the mercuric acetate as a primary reference and setup sample and noted that the multiple isotropic peaks likely resulted from a magic-angle mis-set.[38] Groombridge conducted further experiments on this compound and demonstrated that even a slight mis-setting of the magic angle can result in the appearance of additional peaks, which may spuriously suggest the existence of multiple species.[39] It was further suggested that this would be the case for many heavy metal spin-$^1/_2$ nuclei with large CSAs. Most recently, Wasylishen and co-workers reported the following mercury CSA parameters for mercury(II) acetate: $\delta_{iso} = -2497$ ppm, $\Omega = 1826$ ppm, and $\kappa = 0.90$.[40]

The ^{199}Hg CP/MAS spectrum (Figure 4a) acquired at $\nu_{rot} = 3$ kHz has a manifold of sidebands that resembles previously reported spectra. Unfortunately, this pattern is difficult to analyse correctly by the method of Herzfeld and Berger, since the pattern has a breadth of 130 kHz, is not uniformly excited, and has sideband intensities which may not accurately reflect the mercury CSA. The static ^{199}Hg CP/Hahn-echo and CP/CPMG spectra of $(CH_3COO)_2Hg$ are shown in parts b and c of Figure 4, respectively. Notably, the CP/Hahn-echo spectrum was recorded with 10 times the number of scans used to acquire the CP/MAS and CP/CPMG spectra, and yet its S/N is approximately six times less than that of the corresponding CP/CPMG spectrum. The powder patterns in the ^{199}Hg CP/Hahn-echo and CP/CPMG spectra bear little resemblance to the powder pattern in the CP/MAS spectrum due to the difficulty in uniformly exciting the broad powder pattern over the entire span of the chemical shielding anisotropy (1800 ppm = 128 kHz at 9.4 T).

Because of limitations in the attainable excitation bandwidth, which is dependent upon pulse width and the magnitude of ω_1,[41] as well as orientation-dependent CP efficiency, only a portion of the total powder pattern can be excited. In this case, piecewise wide-line experiments are required to observe the complete line shape (shown in Figure 4d for comparison and described in Figure 5). Acquisition of wide-line solid-state NMR spectra consists of acquiring segments of the spectrum at suitably fixed transmitter frequency intervals over a wide frequency range. Possible methods of combining the data to produce the final wide-line spectrum include (i) recording echo intensities over small intervals and plotting them as a function of frequency (the "point by point" method),[42] (ii) addition,[43] or (iii) skyline projection[7] of Fourier-transformed frequency-domain sub-spectra acquired over a range of evenly spaced offset frequencies. Each of the sub-spectra were acquired using ^{199}Hg CP/CPMG NMR over transmitter increments of 28 kHz (top of Figure 5) and then co-added according to method ii (Figure 5b). For comparison, a skyline projection of the sub-spectra was also constructed (Figure 5c). There is better agreement between the co-added (Figure 5b) and idealized (Figure 5a) powder patterns; the intensity of the high-frequency discontinuity in Figure 5c is diminished considerably. Comparison of methods ii and iii were performed for all reported wide-line spectra against patterns derived from simulations; method iii showed superior results only for the ^{199}Hg wide-line CPMG spectrum (vide infra). The slight "wobble" across the envelope of the wide-line spectra (both added and skyline) results from slight increases in intensity near the center of each pattern (the highest intensity is located at the center of excitation near the transmitter frequency). The spacing of the transmitter offsets and rf field strengths are chosen to minimize this wobble and maximize the uniform excitation of the entire pattern. Use of the CPMG sequence instead of a conventional spin−echo sequence leads to a rapidly collected, high S/N (313) wide-line static ^{199}Hg spectrum. While it is true that acquisition of the ^{199}Hg wide-line CP/CPMG spectrum (Figure 4d) took six times as long as the ^{199}Hg CP/MAS spectrum to acquire (six sub-spectra recorded), the former gives precise chemical shielding tensor information free from the effects of incomplete excitation or variable sideband intensities. The corresponding CP/Hahn-echo experiment would take much

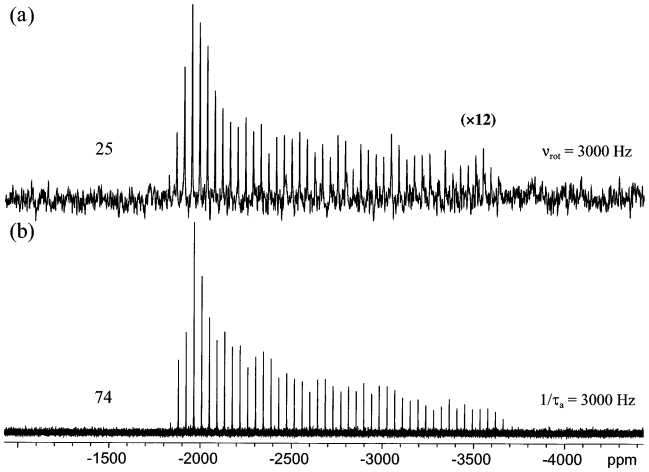

Figure 6. Comparison of the ^{199}Hg (a) MAS at $\nu_{rot} = 3000$ Hz and (b) wide-line CPMG ($1/\tau_a = 3000$ Hz) spectra of $(CH_3COO)_2Hg$; 16 transients were acquired for the MAS spectrum and each of the three CPMG sub-spectra. The CPMG spectrum results from taking the skyline projection of the sub-spectra.

longer to acquire and would be restricted by poor S/N. Mercury CS parameters derived from simulation of the wide-line CP/CPMG spectrum ($\delta_{iso} = -2496$ ppm, $\Omega = 1850$ ppm, $\kappa = 0.87$) agree well with reported values[40] (according to Groombridge, Ω ranges from 1781 ppm for a static sample to 1809−1845 ppm when spinning).[39]

^{199}Hg NMR experiments without the application of cross polarization were also conducted. Static ^{199}Hg wide-line CPMG ($1/\tau_a = 3$ kHz) NMR sub-spectra (three sub-spectra acquired) and the ^{199}Hg MAS ($\nu_{rot} = 3$ kHz) spectrum were recorded with equal overall acquisition times (parts a and b of Figure 6). The purpose of running these experiments is to demonstrate that the CPMG sequence is a viable pulse sequence for obtaining static powder patterns when CP conditions are poor or unavailable and that a broader excitation bandwidth is attainable when directly exciting the observe nucleus. Comparison of the two spectra in Figure 6, which have the same sideband and spikelet separation, demonstrates the large gains in S/N from the CPMG sequence. Only three subspectra were required to reconstruct the entire static ^{199}Hg CPMG spectrum, while comparable S/N in the MAS spectrum would require an increase in the acquisition time by nearly an order of magnitude. It is worth mentioning that both the MAS and CPMG spectra in Figure 6 actually display similar noise levels (MAS spectrum is vertically enhanced by a factor of 12) and that signal accumulation benefits tremendously from using the CPMG sequence for $(CH_3COO)_2Hg$ owing to the very suitable relaxation properties it possesses.

^{207}Pb NMR. ^{207}Pb is an interesting NMR nucleus owing to the immense chemical shift range and large CSAs which result from the easily polarized lead valence orbitals.[36,44] Small changes in molecular structure and local symmetry about the ^{207}Pb nucleus result in significant changes in the characteristics of ^{207}Pb chemical shift tensors.[15] In fact, the changes are so sensitive to structural change that several lead-containing compounds are used as "NMR thermometers" for the calibration of temperatures in NMR probes.[45] ^{207}Pb NMR is of great interest due to the number of technologically relevant materials containing lead,[46] for its application in studying lead speciation in waste disposal media,[26] and for recent involvement in the discovery of a spin-phonon Raman scattering mechanism contribution to spin−lattice relaxation in solids.[47] To our knowledge, solid-state ^{207}Pb NMR spectra of $(CH_3COO)_2Pb{\cdot}3H_2O$ have been

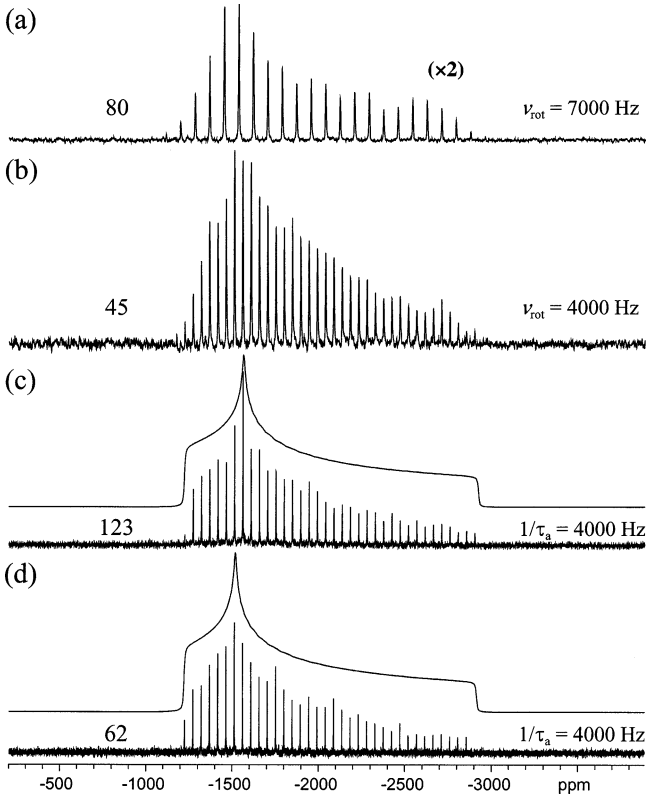

Figure 7. ^{207}Pb (a) MAS ($\nu_{rot} = 7000$ Hz), (b) CP/MAS ($\nu_{rot} = 4000$ Hz), (c) wide-line CPMG and (d) wide-line CP/CPMG ($1/\tau_a = 4000$ Hz) NMR spectra of $(CH_3COO)_2Pb{\cdot}3H_2O$; analytical simulations are shown above corresponding wide-line spectra. For each of the CPMG and CP/CPMG sub-spectra, 64 and 144 transients were respectively acquired.

reported twice before. Harbison and co-workers acquired the static ^{207}Pb NMR spectrum and reported the CS tensor parameters $\delta_{iso} = -1904$ ppm, $\Omega = 1728$ ppm, and $\kappa = 0.62$,[48] while Irwin et al. determined that there is a single magnetically distinct Pb site with an isotropic chemical shift of $\delta_{iso} = -1897$ ppm as well as spinning sidebands covering a breadth of 50 kHz at 4.7 T,[49] corresponding to $\Omega \approx 1190$ ppm by ^{207}Pb CP/MAS NMR.

A series of ^{207}Pb NMR spectra acquired under various conditions are shown in Figure 7. There is a rapid drop off in CP efficiency with higher spinning speeds (even using VACP pulse sequences); therefore, it was more efficient to acquire the ^{207}Pb MAS spectrum at $\nu_{rot} = 7$ kHz without CP. The poor CP efficiency is evidenced by the lower S/N of the CP/MAS spectrum ($\nu_{rot} = 4$ kHz) compared to the MAS spectrum ($\nu_{rot} = 7$ kHz), although the acquisition time of the CP/MAS spectrum was longer by a factor of 5 times (535 and 107 min, respectively). The static piecewise wide-line ^{207}Pb CPMG and CP/CPMG NMR spectra of $(CH_3COO)_2Pb{\cdot}3H_2O$ were acquired with total acquisition times of 107 and 48 min, respectively (parts c and d of Figure 7), and both wide-line spectra display S/N superior to the CP/MAS spectrum. Fitting of the CPMG and CP/CPMG powder patterns (upper traces of parts c and d of Figure 7) yields $\delta_{iso} = -1898$ ppm, $\Omega = 1693$ ppm, $\kappa = 0.60$ and $\delta_{iso} = -1881$ ppm, $\Omega = 1690$ ppm, $\kappa = 0.65$, respectively, in agreement with CS tensor parameters reported by Harbison et al.[48] CS tensor parameters obtained from the ^{207}Pb MAS NMR experiment are also in reasonable agreement with the parameters of Harbison et al. The CP/CPMG sequence is useful for samples such as $(CH_3COO)_2Pb{\cdot}3H_2O$, where spinning might alter the properties of the sample, and for

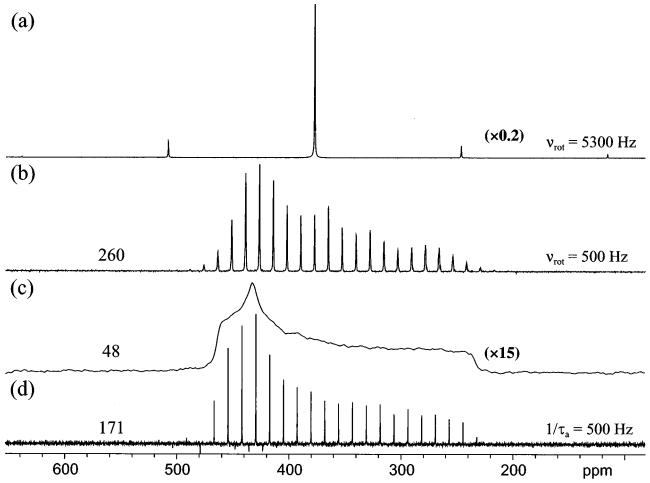

Figure 8. ^{15}N CP/MAS at (a) $\nu_{rot} = 5300$ Hz and (b) $\nu_{rot} = 500$ Hz, (c) CP/Hahn-echo and (d) CP/CPMG ($1/\tau_a = 500$ Hz) NMR spectra of the NO_3 site in doubly 98% ^{15}N-enriched NH_4NO_3 recorded with a total of 16 transients in each case.

samples that are difficult to spin, damaged by spinning, or undergo structural and/or phase changes as a result of small to moderate temperature variations. Furthermore, by acquiring spectra without mechanical spinning, additional peaks due to mis-setting of the magic-angle will be absent.

^{15}N NMR. ^{15}N NMR is of great interest for its applications in studying molecular structure and dynamics in a broad variety of nitrogen-containing systems. Hundreds of nitrogen chemical shift tensors have been measured by standard ^{15}N CP/MAS and static NMR experiments,[15] as well as by combined experimental and theoretical studies on important organic[51] and biological molecules.[52] The application of solid-state ^{15}N NMR is incredibly varied and ubiquitous: recent interesting applications include the study of polypeptides and proteins in membranes,[53] the use of ^{15}N-labeled pyridine as a probe of mesoporous silica surfaces,[54] and natural abundance ^{15}N NMR to study nitrogen sites in nylon-6.[55]

The ^{15}N CP/MAS ($\nu_{rot} = 5300$ and 500 Hz), CP/Hahn-echo, and CP/CPMG spectra of the NO_3 resonance of doubly 98% ^{15}N-enriched ammonium nitrate, which is a solid-state NMR standard for ^{15}N NMR,[27] are presented in Figure 8. Comparison of the spectra show results similar to those mentioned previously for ^{113}Cd, ^{199}Hg and ^{207}Pb. The static CP/CPMG spectrum (Figure 8d) yields comparable S/N to the slow-spinning CP/MAS spectrum (Figure 8b) and is superior to the static CP/Hahn-echo spectrum (Figure 8c), when equal acquisition times are employed (S/N = 171, 260 and 48, respectively). Because of the long spin−lattice relaxation times of the ^{15}N nuclei in this molecule, ^{15}N MAS NMR spectra without CP were not acquired. The NH_4 resonance has a very narrow line width (ca. 10 Hz), making it unsuitable for observation by CPMG-type experiments due to the relatively long T_2* (which when similar in magnitude to T_2, prevents the acquisition of echo trains). In fact, the small negative spikelets observed between the spikelets making up the NO_3 resonance are found to arise from refocusing of the NH_4 magnetization before complete dephasing in the transverse plane (i.e., at a time shorter than the ammonium ^{15}N T_2*). The spikelets interleaved between the nitrate resonance can be removed by allowing enough time for the NH_4 magnetization to fully decay; however, much of the intensity from the NO_3 resonance is lost as well (not shown). The greatest disadvantage of employing CPMG-type experiments lies in the inability to differentiate the isotropic shifts of multiple sites.

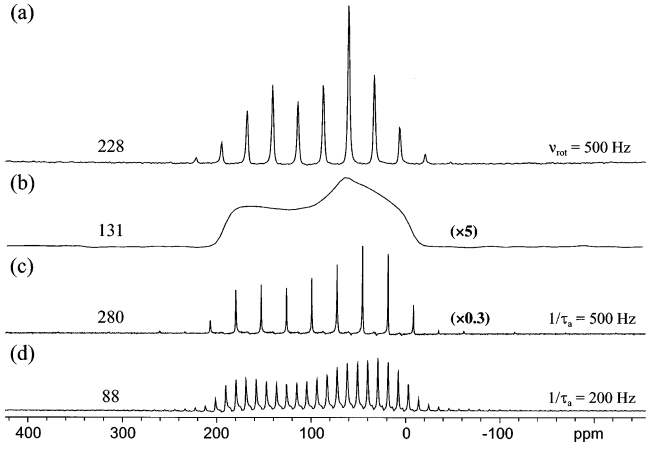

Figure 9. ^{109}Ag (a) CP/MAS ($\nu_{rot} = 500$ Hz), (b) CP/Hahn-echo and CP/CPMG [(c) $1/\tau_a = 500$ Hz, (d) $1/\tau_a = 200$ Hz] NMR spectra of $AgSO_3CH_3$; 480 transients were acquired for all spectra.

However, if samples are singly labeled (often being the case), have only one site of interest, or MAS experiments can be used to identify the isotropic shifts of multiple sites, the CP/CPMG pulse sequence can serve to acquire accurate ^{15}N CS patterns, as evidenced by the parameters presented in Table 1. The ability to obtain a static ^{15}N CP/CPMG powder pattern efficiently (i.e., comparable to CP/MAS) may prove useful for the study of ^{15}N-labeled biological compounds in oriented samples such as membranes.[56]

^{109}Ag NMR. Silver has two NMR active nuclides, ^{107}Ag and ^{109}Ag (n.a. 51.82% and 48.18%, respectively), both of which have small magnetogyric ratios and long spin−lattice relaxation times. ^{109}Ag is favored, since it has a slightly larger γ; however, the NMR frequencies are still so low that many ^{109}Ag NMR experiments suffer from acoustic probe ringing and extremely lengthy experimental times. The first solid-state ^{109}Ag NMR experiments were conducted on microcrystalline powders of silver halides and other simple materials;[57] since then, interesting materials containing silver such as glasses[58] have been investigated by NMR. Because of the aforementioned undesirable characteristics, ^{109}Ag NMR is still largely avoided.

The first ^{109}Ag CP/MAS NMR experiments were conducted on silver acetate and a variety of commercially available silver-containing compounds.[59] A suitable ^{109}Ag CP/MAS standard could not be found at that time, so ^{89}Y CP/MAS NMR of $Y(NO_3)_3 \cdot 6H_2O$ was applied to set the initial conditions for ^{109}Ag−^{1}H Hartmann−Hahn matching due to the proximity of the ^{89}Y Larmor frequency and favorable NMR properties.[60] More recently, $AgSO_3CH_3$ was suggested as a set-up sample for ^{109}Ag CP/MAS experiments.[29] The ^{109}Ag NMR powder pattern is about 4 kHz in breadth at 9.4 T and provides an ideal sample for testing of the CP/CPMG sequence. The ^{109}Ag CP/MAS ($\nu_{rot} = 500$ Hz), CP/Hahn-echo and CP/CPMG NMR spectra of $AgSO_3CH_3$ are shown in Figure 9. Similar to the NH_4NO_3 example, the ^{109}Ag CP/MAS (Figure 9a) and CP/CPMG (Figure 9c) spectra show comparable S/N ratios (228 and 280, respectively), both being far superior to the CP/Hahn-echo spectrum (Figure 9b). Extraction of a precise CSA tensor from either the CP/MAS or CP/CPMG spectra would be difficult, due to the relatively low resolution of these spectra. Acquisition of higher resolution spectra could prove difficult for the standard CP/MAS experiment, since stable spinning speeds of less than 500 Hz on standard NMR probes can be difficult to obtain; however, the needed resolution can easily be obtained using CPMG (Figure 9d). Attempts at recording

spectra for $AgSO_3CH_3$ without CP were unsuccessful owing to the long ^{109}Ag spin−lattice relaxation time.

Conclusions

The CPMG pulse sequence, in combination with CP and TPPM proton decoupling, has been successfully applied to acquire high S/N powder patterns of spin-$^1/_2$ nuclei exhibiting anisotropic chemical shielding patterns. Piecewise CPMG acquisition provides a rapid means of obtaining static NMR spectra of spin-$^1/_2$ nuclei with very broad patterns, which can be analysed to provide accurate chemical shielding tensor parameters unaffected by incomplete excitation or variations in spinning sideband intensities. The manifold of spikelets from CPMG spectra closely resembles the static powder pattern, enabling increasingly accurate analysis of CSA in comparison to the Herzfeld−Berger analysis of MAS spectra (particularly for broad powder patterns). CPMG experiments are ideal for samples that are difficult or impossible to spin, undergo structural and/or phase changes from the stresses of spinning (notably due to temperature change), or even for oriented samples. In addition, signal enhancement of an order of magnitude or more can be attained using CPMG in comparison to conventional static spectra. This allows the acquisition of static spectra with equivalent and possibly better S/N compared to MAS spectra, depending on the spin−lattice and spin−spin relaxation times of the nucleus under observation. The CPMG pulse sequence is useful for samples with spectra that are inhomogeneously and homogeneously broadened; the former is demonstrated in this work and the latter in the ^{29}Si CPMG NMR spectra of Farnan et al.[13] However, the CPMG sequence does suffer from serious drawbacks in that it cannot resolve individual sites based upon their isotropic shifts unless they possess noticeably different CSA patterns or widely dispersed chemical shifts. CPMG also cannot be applied to acquire MAS spectra of spin-$^1/_2$ nuclei at spinning speeds greater than 500 Hz, due to the distribution of signal intensity into sharp sidebands which increases T_2* and significantly decreases (or nullifies) the number of times that the transverse magnetization can be refocused by the CPMG train of π pulses. We hope that the present study will encourage further application of CPMG-type sequences to spin-$^1/_2$ nuclei.

Acknowledgment. This research was funded by Imperial Oil and the Natural Sciences and Engineering Research Council (NSERC, Canada). R.W.S. is also grateful to the Canadian Foundation for Innovation (CFI), the Ontario Innovation Trust (OIT), and the University of Windsor for funding the Solid-State NMR Facility at the University of Windsor. I.H. thanks the Centre for Catalysis and Materials Research (CCMR) at the University of Windsor for a graduate research scholarship. A.J.R. thanks NSERC for an Undergraduate Summer Research Scholarship.

Note Added in Proof. After the submission of this manuscript, we became aware of similar applications of the CPMG sequence (Siegel, R.; Nakashima, T. T.; Wasylishen, R. E. *J. Phys. Chem. B* **2004**, *108*, 2218−2226) to which we refer the reader.

Supporting Information Available: ^{207}Pb NMR spectra of the $(CH_3COO)_2Pb{\cdot}3H_2O$ sample before recrystallization, comparison of ^{15}N Hahn echo, co-added CP/CPMG and CP/CPMG spectra, and addition of ^{207}Pb wide-line CPMG sub-spectra. This material is available free of charge via the Internet at http://pubs.acs.org.

References and Notes

(1) Smith M. E. *Annu. Rep. NMR Spectrosc.* **2001**, *43*, 121−75.
(2) Lipton, A. S.; Sears, J. A.; Ellis, P. D. *J. Magn. Reson.* **2001**, *151*, 48−59.
(3) Larsen, F. H.; Jakobsen, H. J.; Ellis, P. D.; Nielsen, N. C. *J. Phys. Chem. A* **1997**, *101*, 8597−606.
(4) Carr, H. Y.; Purcell, E. M. *Phys. Rev.* **1954**, *94*, 630. (b) Meiboom, S.; Gill, D. *Rev. Sci. Inst.* **1958**, *29*, 688−91.
(5) Lefort, R.; Wiench, J. W.; Pruski, M.; Amoureux, J. P. *J. Chem. Phys.* **2002**, *116*, 2493−501.
(6) Lipton, A. S.; Buchko, G. W.; Sears, J. A.; Kennedy, M. A.; Ellis, P. D. *J. Am. Chem. Soc.* **2001**, *123*, 992−3.
(7) Lipton, A. S.; Wright, T. A.; Bowman, M. K.; Reger, D. L.; Ellis, P. D. *J. Am. Chem. Soc.* **2002**, *124*, 5850−60.
(8) Shore, S. E.; Ansermet, J. P.; Slichter, C. P.; Sinfelt, J. H. *Phys. Rev. Lett.* **1987**, *58*, 953−6. (b) Bryce, D. L.; Gee, M.; Wasylishen, R. E. *J. Phys. Chem. A* **2001**, *105*, 10413−21.
(9) Bryce, D. L.; Wasylishen, R. E. *Phys. Chem. Chem. Phys.* **2003**, *24*, 78−93.
(10) Larsen, F. H.; Jakobsen, H. J.; Ellis, P. D.; Nielsen, N. C. *Mol. Phys.* **1998**, *95*, 1185−95. (b) Larsen, F. H.; Lipton, A. S.; Jakobsen, H. J.; Nielsen, N. C.; Ellis, P. D. *J. Am. Chem. Soc.* **1999**, *121*, 3783−4.
(11) Larsen, F. H.; Nielsen, N. C. *J. Phys. Chem. A* **1999**, *103*, 10825−32.
(12) Schurko, R. W.; Hung, I.; Widdifield, C. M. *Chem. Phys. Lett.* **2003**, *379*, 1−10.
(13) Larsen, F. H.; Farnan, I. *Chem. Phys. Lett.* **2002**, *357*, 403−8.
(14) Harris, R. K.; Sebald, A. *Magn. Reson. Chem.* **1987**, *25*, 1058−62.
(15) Duncan, T. M. *A Compilation of Chemical Shift Anisotropies*; The Farragut Press: Chicago, 1990.
(16) Barrett, S. E.; Durand, D. J.; Pennington, C. H.; Slichter, C. P.; Friedmann, T. A.; Rice, J. P.; Ginsberg, D. M. *Phys. Rev. B* **1990**, *41*, 6283−96.
(17) Waugh, J. S.; Wang, C. H. *Phys. Rev.* **1967**, *162*, 209−17.
(18) Szeverenyi, N. M.; Bax, A.; Maciel, G. E. *J. Magn. Reson.* **1985**, *61*, 440−7.
(19) Lim, K. H.; Nguyen, T.; Mazur, T.; Wemmer, D. E.; Pines, A. *J. Magn. Reson.* **2002**, *157*, 160−2.
(20) Hu, J. Z.; Wind, R. A. *J. Magn. Reson.* **2003**, *163*, 149−62.
(21) Salgado, J.; Grage, S. L.; Kondejewski, L. H.; Hodges, R. S.; McElhaney, R. N.; Ulrich, A. S. *J. Biomol. NMR* **2001**, *21*, 191−208.
(22) Bennett, A. E.; Rienstra, C. M.; Auger, M.; Lakshmi, K. V.; Griffin, R. G. *J. Chem. Phys.* **1995**, *103*, 6951−8.
(23) Bryant, R. G.; Chacko, V. P.; Etter, M. C. *Inorg. Chem.* **1984**, *23*, 3580−4.
(24) Honkonen, R. S.; Doty, F. D.; Ellis, P. D. *J. Am. Chem. Soc.* **1983**, *105*, 4163−8.
(25) Hook, J. M.; Dean, P. A. W.; van Gorkom, L. C. M. *Magn. Reson. Chem.* **1995**, *33*, 77−9.
(26) Fayon, F.; Farnan, I.; Bessada, C.; Coutures, J.; Massiot, D.; Coutures, J. P. *J. Am. Chem. Soc.* **1997**, *119*, 6837−43.
(27) Hayashi, S.; Hayamizu, K. *Bull. Chem. Soc. Jpn.* **1991**, *64*, 688−90.
(28) Witanowski, M.; Stefaniak, L.; Webb, G. A. *Annu. Rep. NMR Spectrosc.* **1993**, *25*, 1.
(29) Penner, G. H.; Li, W. L. *Solid State Nucl. Magn. Reson.* **2003**, *23*, 168−73.
(30) Herzfeld, J.; Berger, A. E. *J. Chem. Phys.* **1980**, *73*, 6021−30.
(31) Summers, M. F. *Coord. Chem. Rev.* **1988**, *86*, 43−134.
(32) Coleman, J. E. In *Metallobiochemistry, Pt D*; Academic Press, San Diego, CA, 1993; Vol. 227, pp 16−43.
(33) Sola, J.; Gonzalezduarte, P.; Sanz, J.; Casals, I.; Alsina, T.; Sobrados, I.; Alvarezlarena, A.; Piniella, J. F.; Solans, X. *J. Am. Chem. Soc.* **1993**, *115*, 10018−28.
(34) Cheung, T. T. P.; Worthington, L. E.; Murphy, P. D.; Gerstein, B. C. *J. Magn. Reson.* **1980**, *41*, 158−68.
(35) Mennitt, P. G.; Shatlock, M. P.; Bartuska, V. J.; Maciel, G. E. *J. Phys. Chem.* **1981**, *85*, 2087−91.
(36) Mason, J. *Multinuclear NMR*; Plenum Press: New York, 1987.
(37) Wrackmeyer, B.; Contreras, R. *Annu. Rep. NMR Spectrosc.* **1992**, *24*, 267−329.
(38) Santos, R. A.; Gruff, E. S.; Koch, S. A.; Harbison, G. S. *J. Am. Chem. Soc.* **1991**, *113*, 469−75.
(39) Groombridge, C. J. *Magn. Reson. Chem.* **1993**, *31*, 380−7.
(40) Eichele, K.; Kroeker, S.; Wu, G.; Wasylishen, R. E. *Solid State Nucl. Magn. Reson.* **1995**, *4*, 295−300.
(41) Schmidt-Rohr, K.; Spiess, H. W. *Multidimensional Solid-State NMR of Polymers*; Academic Press: London, 1995. (b) Fukushima, E.; Roeder, S. B. W. *Experimental Pulse NMR: A Nuts and Bolts Approach*; Addison-Wesley Publishing Company, Inc.: Reading, MA, 1981.

(42) Zhan, P. D.; Prasad, S.; Huang, J.; Fitzgerald, J. J.; Shore, J. S. *J. Phys. Chem. B* **1999**, *103*, 10617−26. (b) Bastow, T. J.; Smith, M. E. *Solid State Nucl. Magn. Reson.* **1992**, *1*, 165−74.

(43) Massiot, D.; Farnan, I.; Gautier, N.; Trumeau, D.; Trokiner, A.; Coutures, J. P. *Solid State Nucl. Magn. Reson.* **1995**, *4*, 241−8. (b) Medek, A.; Frydman, V.; Frydman, L. *J. Phys. Chem. A* **1999**, *103*, 4830−5.

(44) Wrackmeyer, B.; Horchler, K. *Annu. Rep. NMR Spectrosc.* **1990**, *22*, 249−306. (b) Nolle, A. *Z. Naturforsch.* **1977**, *32*, 964−7.

(45) van Gorkom, L. C. M.; Hook, J. M.; Logan, M. B.; Hanna, J. V.; Wasylishen, R. E. *Magn. Reson. Chem.* **1995**, *33*, 791−5. (b) Bielecki, A.; Burum, D. P. *J. Magn. Reson., Ser. A* **1995**, *116*, 215−20.

(46) Dybowski, C.; Neue, G. *Prog. Nucl. Magn. Reson. Spectrosc.* **2002**, *41*, 153−70.

(47) Grutzner, J. B.; Stewart, K. W.; Wasylishen, R. E.; Lumsden, M. D.; Dybowski, C.; Beckmann, P. A. *J. Am. Chem. Soc.* **2001**, *123*, 7094−100.

(48) Kye, Y. S.; Connolly, S.; Herreros, B.; Harbison, G. S. *Main Group Met. Chem.* **1999**, *22*, 373−83.

(49) Irwin, A. D.; Chandler, C. D.; Assink, R.; Hampdensmith, M. J. *Inorg. Chem.* **1994**, *33*, 1005−6.

(50) Van Bramer, S. E.; Glatfelter, A.; Bai, S.; Dybowski, C.; Neue, G. *Concepts Magn. Reson.* **2002**, *14*, 365−87.

(51) Salzmann, R.; Wojdelski, M.; McMahon, M.; Havlin, R. H.; Oldfield, E. *J. Am. Chem. Soc.* **1998**, *120*, 1349−56.

(52) Hu, J. Z.; Facelli, J. C.; Alderman, D. W.; Pugmire, R. J.; Grant, D. M. *J. Am. Chem. Soc.* **1998**, *120*, 9863−9.

(53) Luca, S.; Heise, H.; Baldus, M. *Acc. Chem. Res.* **2003**, *36*, 858−65.

(54) Shenderovich, I. G.; Buntkowsky, G.; Schreiber, A.; Gedat, E.; Sharif, S.; Albrecht, J.; Golubev, N. S.; Findenegg, G. H.; Limbach, H. H. *J. Phys. Chem. B* **2003**, *107*, 11924−39.

(55) Tavares, M. I. B.; de Souza, C. M. G. *J. Appl. Polym. Sci.* **2003**, *90*, 3872−5.

(56) Marassi, F. M. *Concepts Magn. Reson.* **2002**, *14*, 212−24.

(57) Looser, H.; Brinkmann, D. *J. Magn. Reson.* **1985**, *64*, 76−80.

(58) Olsen, K. K.; Zwanziger, J. W. *Solid State Nucl. Magn. Reson.* **1995**, *5*, 123−32.

(59) Merwin, L. H.; Sebald, A. *J. Magn. Reson.* **1992**, *97*, 628−31.

(60) Merwin, L. H.; Sebald, A. *J. Magn. Reson.* **1990**, *88*, 167−71.

(61) Gibby, M. G.; Griffin, R. G.; Pines, A.; Waugh, J. S. *Chem. Phys. Lett.* **1972**, *17*, 80−1.